A COMPARISON OF METHODS FOR SYNTHESIS OF DIRECTIONAL SEAS

M. D. Miles and E. R. Funke
Hydraulics Laboratory
National Research Council of Canada
Ottawa, Ontario, Canada

ABSTRACT

An evaluation of numerical models for the synthesis of directional seas has been carried out in conjunction with the installation of a multi-mode segmented wave generator at the NRC Hydraulics Laboratory. Several authors have recently reported limitations associated with the frequently used double summation model which is neither ergodic nor spatially homogeneous for a finite number of terms. In order to overcome these problems, a modified double summation model is presented which uses unidirectional, narrow-band random wave trains as the fundamental components rather than plane sinusoidal waves. This provides a more realistic representation by reducing the cross correlation of waves from different directions at any given frequency. Various alternatives for generating the fundamental wave trains are investigated by numerical simulation and results are compared to a simpler single summation wave model. Related techniques for computing the required drive signals for a segmented wave machine are also discussed.

1.0 INTRODUCTION

There are now at least 10 major installations throughout the world which are equipped with segmented wave machines capable of generating multi-directional waves [1]. Other installations are expected to follow soon. This fact may have contributed to the recent and growing interest in the methodology of synthesizing multi-directional random sea states.

Much of what is known to date about multi-directional wave generation has grown out of the experience gained over the last 15 years in the simulation of 2-dimensional random waves in wave flumes; an area of endeavour which is still undergoing evolutionary change and still provokes controversy. The added dimension of directionality in multi-directional seas will unquestionably contribute to further discussions. The authors therefore believe it to be helpful to summarize some of the factors which have influenced the evolution of 2-dimensional random wave generation.

From historical background given in [2] and [3], it may be concluded that physical modelling has many limitations which are inherent to the tank and to the wave generating machinery. Nevertheless, in 2-dimensional simulations, under deep water conditions, for moderately high waves, and for wave frequencies up to 0.8 Hz (model scale) it is possible to preserve spectral wave characteristics over considerable propagation lengths of an irregular wave.

However, as waves become steeper and breaking commences, the spectra will undergo a transformation due to instabilities in the course of propagation. This exhibits a typical shift of energy from higher to lower frequencies. The larger waves will also become more non-linear, leading to an interaction of phase-locked and free harmonic components which interact in some areas by cancellation and in other locations by additive superposition. This affects the spectral shape significantly [4]. In addition, the higher frequencies, at least those above 1 Hz, will visibly demonstrate decay through attenuation.

In most physical model studies involving the testing of stationary or nearly stationary structures, these problems are not serious. It is generally possible, through various numerical tools, to tailor the simulation to the client's specifications. This can be done both for spectra as well as for time domain statistics so that, at least in the test area, the simulation matches the expectation. However, when moving vessels are being tested, the requirement to maintain a homogeneous seaway is much more difficult, if not impossible, to achieve under severe sea states.

It is widely accepted that simulations of irregular waves can be adequately represented by the Gaussian assumption. For moderate sea states under deep water conditions, this seems to be satisfactory. However, as the steepness of waves increase, this assumption becomes questionable. Recent work by Myrhaug and Kjeldsen [5] suggests that the Gaussian assumption may not be adequate to describe the properties of large waves in deep water. Nevertheless, the Gaussian model

has served the simulation engineer well until now and moreover, tools for non-linear simulation are not yet generally available. The investigation reported in this paper is therefore based on the Gaussian assumption.

Although physical wave simulation brings along its own set of problems, some of which may overshadow the inadequacies of numerical synthesis techniques, it is nevertheless quite important to understand the limitations of numerical models as they form the input to physical generators. Furthermore, a great deal of research is carried out through numerical simulation in which these tools are being used directly. For this reason, the authors believe that the study presented here is applicable to both areas.

It should be noted that physical and numerical simulation have something in common; it is costly to operate a physical model study over an extended duration and this applies also to numerical modelling. In both situations, there is therefore a motivation to develop models which can achieve adequate simulations within a reasonable length of time, at least to a point when reliable long term behaviour estimates can be made.

For 2-dimensional random wave synthesis, there are three digital computer methods which appear to be commonly used at this time. These are:

- the "random phase" method [6], which has also been referred to as the "deterministic spectral amplitude model" [7]. Its application to the 3-dimensional case shall be called here the RP method for "random phase" method,

- the "random complex spectrum" method [6], which is also known as the "nondeterministic spectral amplitude model" [7] or the "random coefficient scheme" [8] and it shall be known here for the 3-dimensional application as the RFC method for "random Fourier coefficient method ". Finally, there is

- the "filtered white noise" method which will be abbreviated here as the FWN method. For its application to the 3-dimensional case, a distinction is made between narrow band and wide band FWN.

1.1 The Random Phase (RP) Method

In the random phase method, the amplitude of each Fourier component is set deterministically according to the desired spectral density and the phase is set to a random variable with a uniform distribution from $-\pi$ to $+\pi$. The intersample spacing is equal to the inverse of the recycling length of the desired wave train. This amplitude/phase spectrum pair is a polar representation of a complex frequency function and can be readily converted to a time series through the inverse Fourier transform. Although the phases are random, the amplitude spectrum does not usually resemble the spectra normally encountered in nature because the user typically employs one of several parametric model spectra as an input to the method. Sample spectra encountered in nature are quite erratic.

The method can be made to recycle over any length. The only limitation is the capacity of the computer which performs the transform operation. Its main advantage is the fact that the desired spectrum can be guaranteed over the duration of the simulation as long as the sample length is equal to the recycling length of the wave simulation. This method appears to be favoured by those who follow the school of thought that the spectral shape of a simulation must be deterministically defined over the duration of the test.

If the recycling period of the simulation is very long, say for example 10 hours, then individual samples of 20 minute duration will exhibit significant variations in spectral distribution which appear exactly like the spectra for short samples usually encountered in nature. These variations fall within the range of expected statistical variability.

1.2 The Random Fourier Coefficient (RFC) Method

The random Fourier coefficient method is a variant of the RP method. In this technique, a complex spectral function is created synthetically by drawing from Gaussianly distributed random numbers with zero mean and unity variance. These make up the Real and the Imaginary parts of the function. The resultant complex spectrum is identical to that which could have been obtained by Fourier transforming a finite length sample drawn from a white noise source.

The complex spectrum is then multiplied by the square root of the desired spectral density. This operation is equivalent to filtering. A subsequent inverse Fourier transform yields the desired time series. The analogy to the FWN method must be apparent.

Any particular realization of a relatively short duration will exhibit spectral shapes which resemble those seen in nature. If the duration of the simulation is increased while holding the frequency resolution of spectral analysis constant, it will be found that the resulting spectral shape approaches that of the desired (or target) spectral density; a situation which effectively models what may be expected in nature. What may come as a surprise to many newcomers to the business is the fact that the spectral shapes resulting from each short duration realization can deviate very significantly from the target spectral shape.

1.3 The Filtered White Noise (FWN) Method

It is relatively simple to synthesize random number sequences by digital computers which have a uniform or a Gaussian probability distribution. These sequences can be produced with nearly infinite recycling periods and are therefore effectively nonrepetitive. In order to filter these time series in accordance with some predefined spectral characteristics, the user has basically two choices; either

- via the Fourier transform and then by performing the filtering operation in the frequency domain or

- by various time domain operations which are either recursive or non-recursive running average computations.

Although auto-regressive moving average (ARMA) filtering methods [9] can generate time series very efficiently and are generally superior to non-recursive techniques, the ARMA coefficients are difficult to derive for a given spectrum. On the other hand, a filtering operation via the Fourier transform is statistically equivalent to the RFC method.

The application of each of these three basic synthesis techniques has been investigated for the case of multi-directional waves in the context of the double summation wave model.

2.0 DOUBLE SUMMATION WAVE MODELS

The basic double summation model for directional waves is a discrete version of the standard double integral equation for the wave elevation of a random sea with continuous distribution of energy over frequency and angle of propagation [10]. It is given by

$$\eta(x,y,t) = \sum_{i=1}^{N} \sum_{j=1}^{M} A_{ij} \cos[\omega_i t - k_i(x\cos\theta_j + y\sin\theta_j) + \varepsilon_{ij}] \quad (1)$$

where $\omega_i = i(2\pi\Delta f)$, $k_i \tanh(k_i h) = \omega_i^2/g$,

$\theta_j = \theta_0 + j\Delta\theta$ and h = water depth.

The A_{ij}'s and ε_{ij}'s are selected by one of two methods:

Model 1A: $A_{ij} = \sqrt{2S(\omega_i,\theta_j)\Delta\omega\Delta\theta}$ and $\varepsilon_{ij} = 2\pi U[0,1]$ (RP-method).

Model 1B: $A_{ij} = \sqrt{a_{ij}^2 + b_{ij}^2}$ and $\varepsilon_{ij} = \tan^{-1}(b_{ij}/a_{ij})$

where a_{ij} and b_{ij} are Gaussian random variables with variance $S(\omega_i,\theta_j)\Delta\omega\Delta\theta$ (RFC-method).

The wave field is thus a superposition of M two-dimensional wave trains propagating in M different directions with each individual wave train having either RP or RFC properties. This double summation model has been used quite extensively for directional wave simulation but several authors [11,12,13] have reported difficulties with it. The two basic problems are that the resultant wave field is neither ergodic nor spatially homogeneous for finite values of N and M regardless of the record length used. As pointed out by Jefferys [14], these effects are caused by artificial phase locking in any particular realization due to components travelling in different directions with identical frequencies. The wave energy in any one frequency band will therefore typically vary over space from approximately 0 to 4 times its average value regardless of how many directions are used.

We shall consider the case where Δf is the frequency resolution required in the measured point spectrum $S(f)$. This depends on the shape of the wave spectrum and the frequency response of the object being tested but it is typically 0.02 to 0.05 Hz in model basin applications. The problem in applying equation 1 directly at Δf is that all energy in a cell of finite size Δf by $\Delta\theta$ is represented by a single sinusoid. Within Δf, energy from different directions is totally phase locked in any given realization whereas in nature it is uncorrelated. A more realistic version of the double summation model is therefore given by

$$\eta(x,y,t) = \sum_{i=1}^{N} \sum_{j=1}^{M} A_{ij}\, \phi_{ij}(x,y,t) \quad (2)$$

where $A_{ij} = \sqrt{S(\omega_i,\theta_j)\,\Delta\omega\Delta\theta}$

and ϕ_{ij} is a unidirectional narrow-band random (or pseudo random) wave train travelling in direction θ_j with centre frequency ω_i, bandwidth $\Delta\omega$ and unit variance. There are several reasonable ways to choose the ϕ_{ij}'s. In each case, the aim is to make ϕ_{ij} as uncorrelated as possible with ϕ_{im} unless $m = j$. The following three wave models are considered.

Model 2A:

$$\phi_{ij} = \sqrt{\frac{2}{P}} \sum_{\ell=1}^{P} \cos[\omega_{i\ell} t - \alpha_{ij\ell} + \varepsilon_{ij\ell}] \quad (3)$$

where $\omega_{i\ell} = (\omega_i - \Delta\omega/2) + \ell(\Delta\omega/P)$,

$\alpha_{ij\ell}(x,y) = k_{i\ell}(x\cos\theta_j + y\sin\theta_j)$

and $\varepsilon_{ij\ell} = 2\pi U[0,1]$.

Model 2B:

$$\phi_{ij} = \frac{1}{\sqrt{P}} \sum_{\ell=1}^{P} [a_{ij\ell}\cos(\omega_{i\ell}t - \alpha_{ij\ell}) + b_{ij\ell}\sin(\omega_{i\ell}t - \alpha_{ij\ell})] \quad (4)$$

where $a_{ij\ell}$ and $b_{ij\ell}$ are independent Gaussian variables with zero mean and unit variance.

Model 2C:

ϕ_{ij} = Gaussian white noise filtered in the time domain by a narrow band linear filter with centre frequency ω_i, bandwidth $\Delta\omega$ and phase lag $k(x\cos\theta_j + y\sin\theta_j)$.

Other choices are also possible. The frequencies within each ϕ_{ij} could be chosen at random over a bandwidth $\Delta\omega$, for example. This method is not computationally attractive, however, because it precludes direct use of FFT techniques.

When equations 3 and 4 are substituted into (2), the RP and RFC versions of the standard double summation model are obtained at a finer frequency resolution of $df = \Delta f/P$. If the waves are analysed at resolution Δf, models 2A and 2B are therefore equivalent to using frequency averaging on models 1A and 1B which will improve ergodicity and spatial homogeneity as shown by Jefferys [14]. Although 2A and 2B will give more realistic wave fields than model 1, they are still non-ergodic and non-homogeneous for any finite P. Model 2C, on the other hand, is ergodic and homogeneous because the component wave trains are uncorrelated and it should therefore generate the most realistic simulation of a natural sea state.

The behaviour of the variance and cross spectra of wave fields generated by each of the three models was investigated by numerical simulation. In all cases, a target spectrum of the form $S(f)D(f,\theta)$ was used where the spreading function D is defined by

$$D(f,\theta) = C(s)\left|\cos\left[\frac{\pi(\theta-\theta_0)}{2\theta_{max}}\right]\right|^{2s} \quad (5)$$

where $C(s)$ is a normalization factor and the spreading index s may be a function of f. θ_{max} was usually set at $\pi/2$. See [15] for detailed derivations of the equations given in the following sections.

2.1 Distribution of Variance

The most fundamental quantity for evaluating the behaviour of the various wave models is the variance of η either within a frequency band of $\Delta\omega$ or over all frequencies. Let $\hat{\sigma}^2$ denote the variance of a particular realization defined as

$$\hat{\sigma}^2 = \lim_{T\to\infty} \frac{1}{T} \int_0^T \eta^2(x,y,t)\, dt. \tag{6}$$

By considering the ensemble averages for the standard double summation model, it can be shown that

$$\mathrm{Var}[\hat{\sigma}^2] = \frac{1}{4} \sum_{i=1}^{N} \sum_{j=1}^{M} \left[\left\{ \sum_{\ell=1}^{M} A_{ij}^2 A_{i\ell}^2 \right\} - A_{ij}^4 \right]. \tag{7}$$

For Model 1A and large N and M, this becomes

$$\mathrm{Var}[\hat{\sigma}^2] = \Delta\omega \int_0^{\infty} \left\{ S^2(\omega) \left[1.0 - \Delta\theta \int_0^{2\pi} D^2(\omega,\theta)\, d\theta \right] \right\} d\omega. \tag{8}$$

This is similar to an expression derived by Pinkster [13] except for the second term involving the spreading function. In the limiting case of a very narrow spreading function, $D(\omega,\theta)$ tends to a Dirac delta function in θ so equation 8 gives $\mathrm{Var}[\hat{\sigma}^2] = 0$ for any $\Delta\omega$ which corresponds to the unidirectional RP case. For normal directional spreading functions, the second term is quite small for $M > 20$ so equation 8 agrees with Pinkster's expression for large M. Thus, equation 8 shows that the variance of $\hat{\sigma}^2$ is only weakly dependent on the number of angles used. The only effective way to decrease the variance is to decrease $\Delta\omega$ and model 1A becomes ergodic in the limit as $N \to \infty$.

Let $\hat{\sigma}_i^2$ denote the variance of η within the frequency band from $\omega_i - \Delta\omega/2$ to $\omega_i + \Delta\omega/2$. It can be shown for Model 2A that

$$\mathrm{Var}[\hat{\sigma}_i^2] = \frac{1}{P} \left[1.0 - \Delta\theta^2 \sum_{j=1}^{M} D^2(\omega_i,\theta_j) \right]. \tag{9}$$

As before, the second term is small for normal spreading widths when $M > 20$ so the variance of $\hat{\sigma}_i^2$ is also only weakly dependent on M except in the limiting case of unidirectional waves where $\mathrm{Var}[\hat{\sigma}_i^2] = 0$ for any P. Thus, for $M > 20$, $\hat{\sigma}_i^2$ has approximately a chi-square distribution with 2P degrees of freedom. Since the phase of each component of η is linear in both ε and $\vec{x}$, equation 9 applies to both ensemble and spatial averages. Model 2A can therefore be made as ergodic and homogeneous as desired by using a sufficiently large number of sub-frequencies but the computation time may become prohibitive.

It was found by numerical simulation that model 2B has larger variance than 2A for small values of M but both models have essentially the same variance statistics when M is greater than 20.

2.2 Distribution of Cross Spectra

The cross spectra between the wave elevations at various spatial positions are fundamental to many methods which are currently in use for measuring the directional wave spectrum in a basin. It was therefore decided to also compare the wave synthesis models on the basis of the cross spectral density of the wave elevation at two arbitrary points, p and q. For the continuous case [16], this is given by

$$S_{pq}(\omega) = S(\omega) \int_0^{2\pi} D(\omega,\theta)\, \exp\left[i\vec{k} \cdot (\vec{x}_p - \vec{x}_q) \right] d\theta. \tag{10}$$

Let $S_{pq}(\omega) = C_{pq}(\omega) + i\, Q_{pq}(\omega)$ where C_{pq} is the co-spectrum and Q_{pq} is the quad-spectrum. Considering the cross spectrum for model 2A at frequency $\omega = \omega_i$ and dropping the subscript i, it follows that

$$C_{pq} = \frac{S(\omega)\Delta\theta}{P} \sum_{j=1}^{M} \sum_{\ell=1}^{M} \sqrt{D_j D_\ell} \sum_{m=1}^{P} \left[\cos(\varepsilon_{\ell m} - \varepsilon_{jm}) \cos \gamma_{m\ell} + \sin(\varepsilon_{\ell m} - \varepsilon_{jm}) \sin \gamma_{m\ell} \right] \tag{11}$$

where $\gamma_{m\ell} = k(\omega_m) \left[(x_q - x_p)\cos\theta_\ell + (y_q - y_p)\sin\theta_\ell \right]$.

and $D_j = D(\omega,\theta_j)$ where it is assumed that D is constant over a bandwidth of $\Delta\omega$. The expected value of C_{pq} is obtained by averaging over all realizations. Thus,

$$E[C_{pq}] = \frac{S(\omega)\Delta\theta}{P} \sum_{j=1}^{M} D_j \sum_{m=1}^{P} \cos(\gamma_{mj}). \tag{12}$$

Using the relation that $\mathrm{Var}[z] = E[z^2] - E^2[z]$ for any random variable z, it can be shown that the ensemble variance of C_{pq} is given by

$$\mathrm{Var}[C_{pq}] = \frac{S^2(\omega)\Delta\theta^2}{2P^2} \sum_{j=1}^{M} \sum_{\substack{\ell=1 \\ \ell\neq j}}^{M} D_j D_\ell \sum_{m=1}^{P} \left[1.0 + \cos(\gamma_{m\ell} + \gamma_{mj}) \right]. \tag{13}$$

If $\Delta\omega$ is small, then $k(\omega_m) = k(\omega)$ and thus $\mathrm{Var}[C_{pq}] = S^2(\omega) * CV/P$

where $CV = \frac{\Delta\theta^2}{2} \sum_{j=1}^{M} \sum_{\substack{\ell=1 \\ \ell\neq j}}^{M} D_j D_\ell \left[1.0 + \cos(\gamma_j + \gamma_\ell) \right]$ (14)

and $\gamma_j = k(\omega) \left[(x_q - x_p)\cos\theta_j + (y_q - y_p)\sin\theta_j \right]$.

In a similar manner, it follows that $\mathrm{Var}[Q_{pq}] = S^2(\omega) * QV/P$

where $QV = \frac{\Delta\theta^2}{2} \sum_{j=1}^{M} \sum_{\substack{\ell=1 \\ \ell\neq j}}^{M} D_j D_\ell \left[1.0 - \cos(\gamma_j + \gamma_\ell) \right]$. (15)

CV and QV are functions of $(\vec{x}_p - \vec{x}_q)$, $D(\omega,\theta)$ and M. For parametric spreading functions such as equation 5, CV and QV are therefore functions of R/L, ψ, M and s where R is the distance between points p and q, ψ is the angle from p to q relative to the x-axis, s is the spreading index and L is the wavelength corresponding to frequency ω. CV and QV are plotted in Figures 1 to 4 for typical ranges of these parameters. It can be seen from Figure 1 that CV and QV are only weakly dependent on M for M greater than 20 and so C_{pq} and Q_{pq} are similar to $\hat{\sigma}_i^2$ in this respect. CV and QV are always less than or equal to 1 and generally lie between 0.2 and 0.8. The magnitudes of C_{pq} and Q_{pq} therefore have approximately chi-square distributions with C*P degrees of freedom where C is a constant of order 1.

For large M and N, we obtain

$$\mathrm{Var}\begin{bmatrix} C_{pq} \\ Q_{pq} \end{bmatrix} = \frac{S^2(\omega)}{2P}\left\{1.0 \pm \frac{|S_{pq}(\omega)|^2}{S^2(\omega)}\cos(2\phi_{pq}(\omega))\right.$$

$$\left. -\Delta\theta \int_0^{2\pi} D^2(\omega,\theta)\left[1.0 \pm \cos(2\gamma)\right] d\theta\right\} \qquad (16)$$

where ϕ_{pq} = phase of S_{pq}

and $\gamma = k(\omega)\left[(x_q - x_p)\cos\theta + (y_q - y_p)\sin\theta\right]$.

The last term in equation 16 is similar to the last term in equation 8 and is usually quite small for typical spreading functions. It can be seen that equation 16 reduces to equation 9 when p=q and that the variance of C_{pq} and Q_{pq} tends to zero as it should in the limiting case of unidirectional waves.

The cross spectrum for a particular realization of model 2B is given by

$$S_{pq}(\omega) = \frac{S(\omega)\Delta\theta}{2P}\sum_{j=1}^{M}\sum_{\ell=1}^{M}\sqrt{D_j D_\ell}\sum_{m=1}^{P}\{ \qquad (17)$$

$$\left[(a_{jm}a_{\ell m}+b_{jm}b_{\ell m})\cos\gamma_{j\ell m}+(a_{jm}b_{\ell m}-b_{jm}a_{\ell m})\sin\gamma_{j\ell m}\right]$$

$$+ i\left[(a_{jm}a_{\ell m}+b_{jm}b_{\ell m})\sin\gamma_{j\ell m}-(a_{jm}b_{\ell m}-b_{jm}a_{\ell m})\cos\gamma_{j\ell m}\right]\}$$

where $\gamma_{j\ell m} = \alpha_{jm}(\vec{x}_p) - \alpha_{\ell m}(\vec{x}_q)$

and $\alpha_{jm}(\vec{x}) = k(\omega_m)[x\cos\theta_j + y\sin\theta_j]$.

This equation was used to calculate the ensemble variability of model 2B cross spectra by simulation for comparison with the model 2A variability as given by equations 14 and 15. A typical result for M = 30 is shown in Table 1. In general, it was found that models 2A and 2B have essentially the same variability when M is greater than 20 or so. This result can be explained as follows. The cross spectrum of any realization is a function of the a and b coefficients of the Fourier transform of the wave elevation formed by adding wave trains from M directions. At each frequency, a and b are therefore the sum of M independent random variables. By the central limit theorem, they will have a Gaussian distribution under fairly general conditions regardless of the statistical distributions of the a's and b's in each component wave train. Thus, models 2A and 2B are statistically equivalent except for small M. This result is in contrast to the two dimensional case where the RP and RFC models give completely different statistics [17]. It also supports Goda's contention [18] that the RP method should correctly reproduce the statistical variability of natural multi-directional waves.

2.3 Effects of Finite Record Length

The variances and cross spectra considered so far are based on wave records of infinite length. In this situation, model 2C is clearly superior to models 2A and 2B since it produces cross spectra with zero variability. The relative behaviour of the models must also be compared at the finite record lengths required by practical applications, however.

Since models 2A and 2B are periodic, the results given in section 2.2 also apply for a finite record length T if P is set equal to Δf^*T. The distribution of cross spectra for model 2C was investigated by numerical simulation.

If the discrete Fourier transform of a finite segment of a FWN signal is computed, the coefficients will be Gaussianly distributed about their mean value. In this sense, one would expect model 2C to behave in a similar manner to model 2B for finite length records. Time domain synthesis does differ from model 2B in at least two respects, however. The cardinal filter implicit in 2B is not physically realizable in the time domain and FFT synthesized records are always cyclic whereas segments of filtered white noise are not. In order to assess the significance of these effects, model 2C was simulated using the following procedure.

For reasons of computational efficiency, the narrow band noise signals were synthesized by the RFC method using the following spectral density:

Given $\xi = \pi(f - fc)/fw$,

$$S(f) = \left[\cos(\xi)^*\left|\cos(\xi)\right|^{\alpha-1} + 1.\right]/2.$$

for $fc-fw < f < fc+fw$

$= 0$ everywhere else.

This function is illustrated in Figure 5 for fc = 0.5 Hz, fw = 0.04 Hz and α = 0.5. A frequency spacing of 1/1638.4 Hz was used.

In order to eliminate the cyclical property of the noise signal, only 95% of the record was used for subsequent statistical analysis. Cross-correlation coefficients between the first and the subsequent 9 of 10 realizations varied from 0.191 to 0.266.

The narrow band wave trains were synthesized for each of M directions and were then transposed and summed to obtain the total wave elevation at two positions. Standard FFT techniques based on segment averaging with a Parzen data window were then used to calculate the cross spectrum for each realization of model 2C.

Typical results are shown in Table 2 and it can be seen that model 2C has somewhat smaller variability than model 2A for a given record length. This difference is probably due mainly to the shape of the filter since the standard Blackman and Tukey relation [19] gives an effective bandwidth of 1.22 Δf for the filter used in model 2C compared to Δf for the rectangular filter implicit in model 2A. The spectral variance of the narrow band wave trains should thus be 18% less for model 2C which is consistent with the results in Table 2.

All three models thus have similar statistical behaviour on finite length records for M greater than 20 and any one of them should provide a realistic simulation of a finite time segment of a natural sea state within the range of linear wave theory. It therefore appears that the only effective way to reduce spatial variability with the double summation model is to increase record length. This requires very long test times compared to two dimensional testing. At a scale of 1:40, for example, a model test period of 4 minutes corresponds to 25 minutes full scale. As can be seen from Figure 6, the average wave energy over this period in a band of 0.04 Hz varies from 0.3 to 1.3 depending on spatial position. This is not considered unrealistic and we expect that a similar variation would be observed in a full scale situation over the same period

of time. Thus, testing times must be very long to properly cover all situations. For example, about 7 hours model (or 44 hours full scale) would be needed to reduce the spatial variation of energy within this band to ± 5 percent. Such a test would represent the long term average for a given spectrum rather than a single continuous record since the sea is seldom statistically stationary for more than a few hours at a time.

2.4 Synthesis of Wave Generator Drive Signals

In principle, the narrow band FWN method could be used to synthesize drive signals for a segmented wave generator in the time domain but it would be computationally intensive because of the filtering required to propagate each component wave train to each segment of the wave machine. One way to reduce the computation time would be to exploit the narrow band property and replace the filtering with a time shift based on the phase velocity of the centre frequency. This technique was investigated but it was found to be a useful approximation only at relatively low frequencies. Therefore, it will normally be more efficient to synthesize in the frequency domain using a procedure such as the following which is equivalent to model 2B.

Let $Z_n(\omega)$ be the Fourier transform of the drive signal for the wave board motion of segment n. Z is computed as follows:

$$Z_n(\omega) = \sum_{j=1}^{M} H_{nj}(\omega)\Phi_j(\omega) \qquad (18)$$

where $\Phi_j(\omega)$ is the Fourier transform of a long-crested wave train generated by the RFC method for a target spectrum of $S(\omega)D(\omega,\theta_j)\Delta\theta$. The recycling period is set to P/Δf where P is selected by equations 9, 14 and 15 for the required degree of spectral variability.

$H_{nj}(\omega)$ is a filter relating the wave board motion of segment n to the wave elevation at the basin reference position for a sinusoidal wave component with frequency ω and direction θ_j. The H_{nj}'s can be precomputed and stored on disk since they only depend on M and the position of the basin reference point.

Thus, only one inverse FFT is required per segment. If desired, the point spectrum can be calculated for each realization and used to rescale the Φ_j's so that the target spectrum will be obtained at resolution Δf. This normalization can only be done at one position in the basin, however.

3.0 SINGLE DIRECTION PER FREQUENCY MODELS

Another approach to synthesizing a directional sea is to use a model in which each sinusoidal component has a unique frequency which is resolvable in a finite record length, T. This will produce a spatially homogeneous wave field because all cross product terms will average to zero regardless of the direction of propagation of each component. One such method is the single summation model defined by

$$\eta(x,y,t) = \sum_{i=1}^{N} A_i \cos[\omega_i t - k_i(x\cos\theta_i + y\sin\theta_i) + \varepsilon_i] \qquad (19)$$

where $\omega_i = i(\Delta\omega/M)$. The θ_i are chosen by some scheme such that all M angles are included in each frequency band of width Δω. A_i and ε_i are selected using either the RP or the RFC method.

Sand [3] has described a variation on this method in which two directions per frequency are included by using components which are 90 degrees out of phase. Although it is ergodic at the reference point, this model does not seem to be spatially homogeneous because the phase condition can only be enforced at one position for any particular realization. Consequently, only the single direction per frequency case is considered here.

We define wave model 3 as a particular implementation of the single summation method in which $\theta_i = ((i-1) \bmod M)\Delta\theta - \theta_{max}$ where $\Delta\theta = 2\theta_{max}/(M-1)$. The discrete components are thus distributed on a spiral in the ω,θ plane in contrast to the circular distributions of the standard double summation model as shown in Figure 7. If we further consider the RP case and also keep A_i constant over bandwidth Δω, then wave model 3 can be written in the form of equation 2 where

$$\phi_{ij} = \sqrt{2}\cos[\omega_{ij}t - k_{ij}(x\cos\theta_j + y\sin\theta_j) + \varepsilon_{ij}] \qquad (20)$$

and $\omega_{ij} = (i - 1/2 + j/M)\Delta\omega$.

Thus, the wave field is a superposition of M long-crested wave trains. Each wave train contains N frequencies at spacing Δω but they are shifted so that no pair of wave trains contain the same frequencies. The spectrum of the synthesized waves is equal to the target spectrum at all spatial positions for record length T where $T = M/\Delta f$. Thus, unlike models 2A and 2B, the recycling period of model 3 is related to the number of wave angles.

Although the frequency spacing is clearly artificial, the wave field should become realistic for sufficiently large M and sufficiently small Δω. How large M must be for a given Δf will probably depend on the type of model test being conducted. Some indication of the minimum acceptable value may be obtained by considering the differences between the cross spectra of waves generated by model 3 and the actual cross spectra for the continuous target spectrum defined by equation 10. The amplitude and phase errors were computed as functions of M, s, R/L and ψ and are shown in Figures 8 to 11. It can be seen that the cross spectra will be reasonably accurate for M > 32 over the normal ranges of the other parameters.

If the primary aim is to generate the target directional spectrum at all points in the test area, model 3 has definite advantages compared to the previous models. At Δf = 0.04 Hz and M = 32, a testing time of 13 minutes is required whereas model 2C would require about 90 minutes to keep the spatial variability of the spectral density within ± 10 percent. Model 3 must be used with caution when testing nonlinear devices, however, since the maximum wave heights may tend to be smaller than those which could occur on a particular realization of a real sea over the same time period.

4.0 CONCLUSIONS

The double summation method can be used to synthesize realistic multi-directional seas if P frequency components are included in a band width Δf where Δf is the required frequency resolution and P is sufficiently large to reduce the variability of the cross spectra to an acceptable level. In contrast to the unidirectional case, the RP and RFC methods both produce statistically similar waves when the number of wave directions

exceeds 20. The variability of the cross spectra depends only weakly on the number of wave directions and the only effective way to reduce it is to increase the record length. The required test duration is inversely proportional to Δf and thus depends on the shape of the wave spectrum and the frequency response of the object being tested; i.e. the smaller the damping, the smaller should be Δf. Test durations will generally be much longer than those required for unidirectional waves.

The single summation method can generate spatially homogeneous seas with much shorter record lengths than the double summation method. The cross spectra will be reasonably accurate if at least 30 wave directions are used. However, this method must be employed with caution when testing nonlinear devices because the variability is not commensurate with natural seas of the same duration.

5.0 REFERENCES

1. Miles, M.D., Laurich, P.H. and Funke, E.R., "A Multi-mode Segmented Wave Generator for the NRC Hydraulics Laboratory", Proc. 21st American Towing Tank Conference, Washington D.C., August, 1986.

2. Funke, E.R., "A Rationale for the Use of the Deterministic Approach to Laboratory Wave Generation", Paper presented to the Joint Seminar of the IAHR Working Group on Wave Generation and Analysis and the International Towing Tank Conference, Delft, Holland, October 31st, 1986.

3. Sand, S.E., "Directional Wave Generation". Paper presented to the Joint Seminar of the IAHR Working Group on Wave Generation and Analysis and the International Towing Tank Conference, Delft, Holland, October 31st, 1986.

4. Sand, S.E. and Mansard, E.P.D., "Description and Reproduction of Higher Harmonic Waves", National Research Council of Canada, Hydraulics Laboratory Technical Report, TR-HY-012, January, 1986.

5. Myrhaug, D. and Kjeldsen, S.P., "Steepness and Asymmetry of Extreme Waves and the Highest Waves in Deep Water.", to be published in Ocean Engineering after June, 1986.

6. Funke, E.R. and Mansard, E.P.D., "The NRCC 'Random' Wave Generation Package", National Research Council of Canada, Hydraulics Laboratory Technical Report, TR-HY-002, March, 1984.

7. Tuah, H. and Hudspeth, R.T., "Comparison of Numerical Random Sea Simulations", J. of Waterway, Port, Coastal & Ocean Divis., ASCE, Vol. 108, No. WW4, Proc. Paper 17488, November, 1982, pp. 569-584.

8. Elgar, S., Guza, R.T. and Seymour, R.J., "Wave Group Statistics from Numerical Simulations of a Random Sea", Applied Ocean Research, Vol.7, No.2, 1985.

9. Samii, K. and Vandiver, J.K., "A Numerically Efficient Technique for the Simulation of Random Wave Forces on Offshore Structures", Paper No. OTC-4811, 16th OTC, Houston, TX, 1984.

10. Pierson, W.J., Jr., "Wind-generated Gravity Waves", in Advances in Geophysics, Vol.2, New York: Academic Press, Inc., 1955, pp. 93-178.

11. Forristall, G.Z., "Kinematics of Directionally Spread Waves", Proc. Directional Wave Spectra Applications, Univ. of Berkeley, 1981, pp. 129-146.

12. Lambrakos, K.F., "Marine Pipeline Dynamic Response to Waves from Directional Spectra", Journal Ocean Engineering., Vol.9, No. 4, 1982, pp. 385-405.

13. Pinkster, J.A., "Numerical Modelling of Directional Seas", Proc. Symposium on Description and Modelling of Directional Seas, Tech. Univ. of Denmark, Copenhagen, 1984, No. C-1-11.

14. Jefferys, E.R., "Directional Seas should be Ergodic", to be published in Applied Ocean Research July 1987, Vol. 9, No. 3.

15. Miles, M.D., "Numerical Models for Synthesis of Directional Seas", National Research Council of Canada Hydraulics Laboratory Technical Report TR-HY-016, 1986.

16. Isobe, M., Kondo, K. and Horikawa, K., "Extension of MLM for Estimating Directional Wave Spectrum", Proc. Symposium on Description and Modelling of Directional Seas, Tech. Univ. of Denmark, Copenhagen, 1984, No. A-6-1.

17. Tucker, M.J., Challenor, P.G. and Carter, D.J.T., "Numerical Simulation of a Random Sea: A Common Error and its Effect upon Wave Group Statistics", Applied Ocean Research, Vol. 6, No. 2, 1984.

18. Goda, Y., "Simulation in Examination of Directional Resolution", Proc. Directional Wave Spectra Applications, Berkeley, September 1981, pp. 387-407.

19. Blackman, R.B. and Tukey, J.W., "The Measurement of Power Spectra from the Point of View of Communications Engineering", Dover Publications, Inc., New York, 1958, Chapter 8.

Table 1
Measured Variability of Model 2B Cross Spectra

(M = 30, s = 1.0, fo = 1.0 Hz, Δf = 0.04 Hz, 500 Realizations)				
P	Theoretical Std. Dev. (Model 2A)		Measured Std. Dev. (Model 2B)	
	Cpq	Qpq	Cpq	Qpq
10	0.1916	0.2418	0.1923	0.2353
100	0.0606	0.0765	0.0605	0.0790
200	0.0428	0.0541	0.0429	0.0544

Table 2
Finite Time Cross Spectra Variability
(Measured Standard Deviation)

(M = 17, s = 1.0, Record Length = 1638 sec, R/L = 0.25, ψ = 45 deg, 200 Realizations)			
	Model 2A	Model 2B	Model 2C
Cpq	0.0812	0.0785	0.0721
Qpq	0.0914	0.0901	0.0857

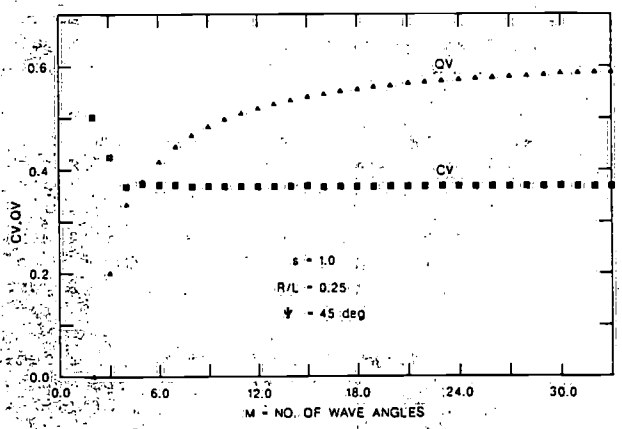

Fig.1 CV and QV versus M for Model 2A.

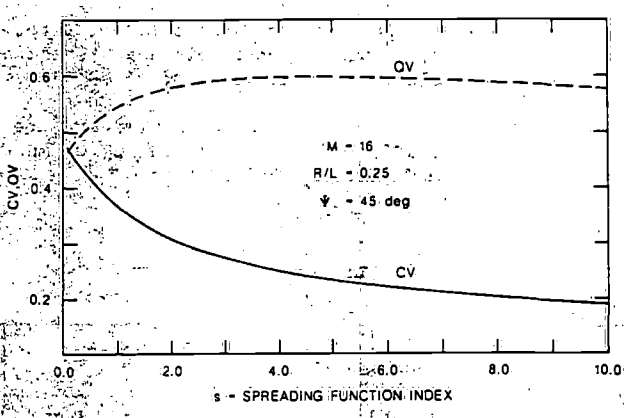

Fig.2 CV and QV versus s for Model 2A.

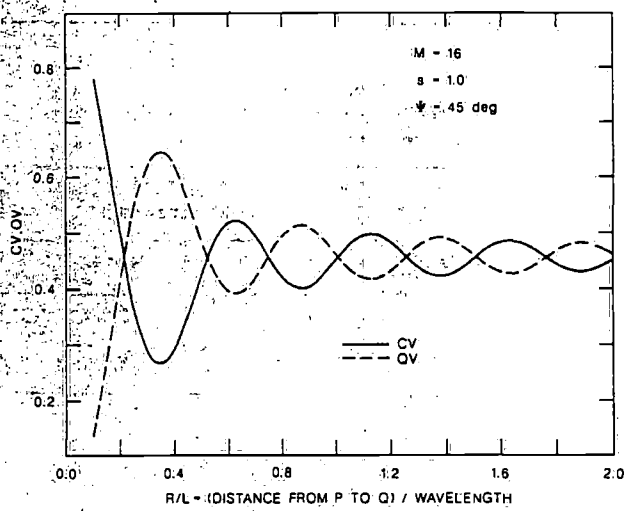

Fig.3 CV and QV versus R/L for Model 2A.

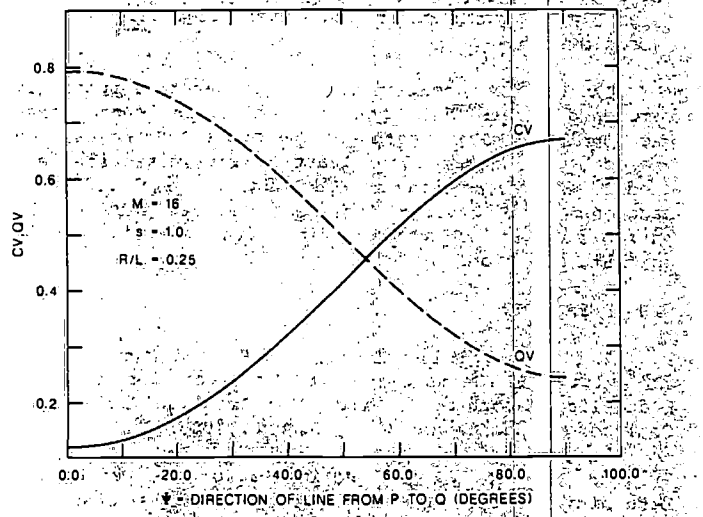

Fig.4 CV and QV versus Ψ for Model 2A.

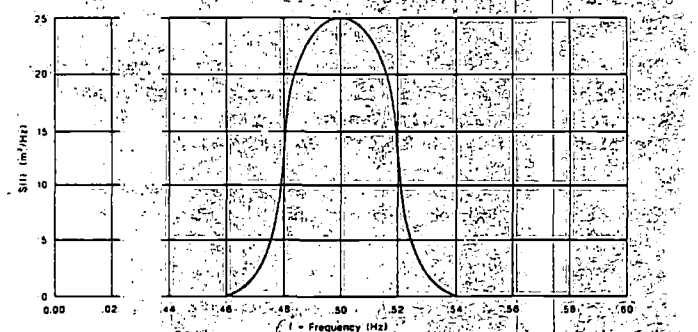

Fig.5 Target Spectral Density for Narrow Band Filtered Noise

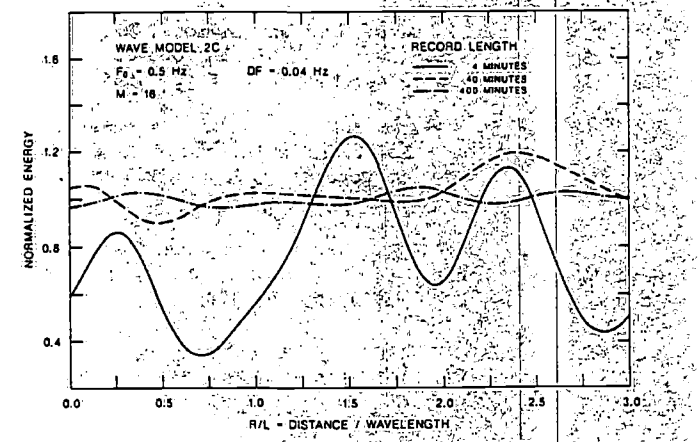

Fig.6 Spatial Variation of Wave Energy in Bandwidth of 0.04 Hz centered at 0.5 Hz.

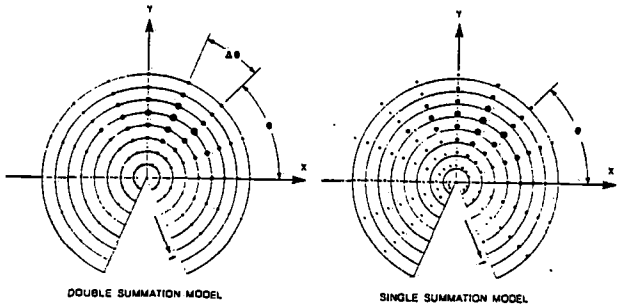

Fig.7 Polar Representation of Double and Single Summation Wave Models.

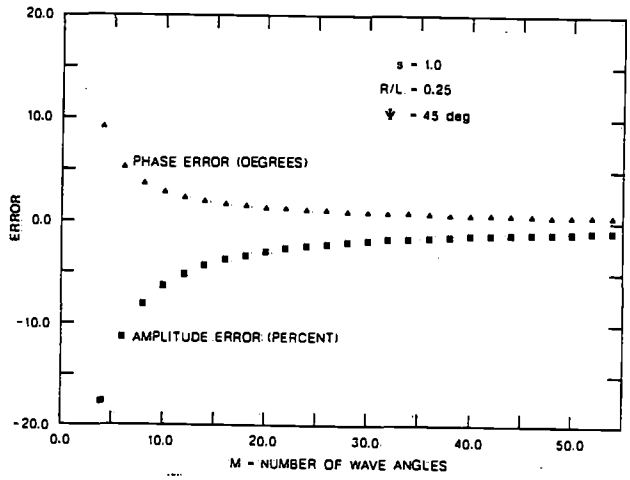

Fig.8 Cross Spectrum Errors for Wave Model 3 versus M.

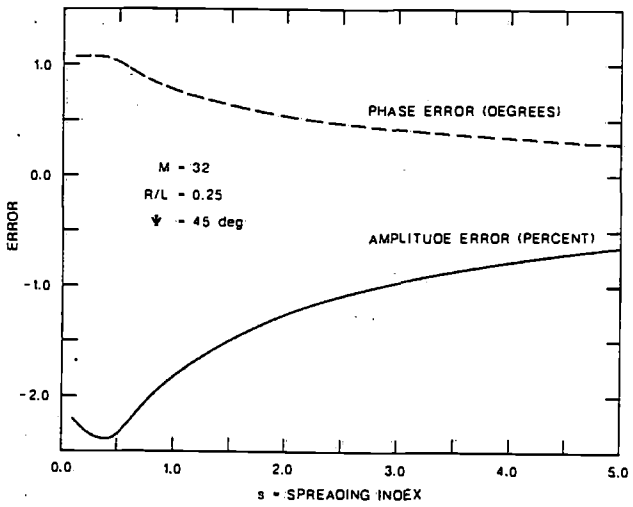

Fig.9 Cross Spectrum Errors for Wave Model 3 versus s.

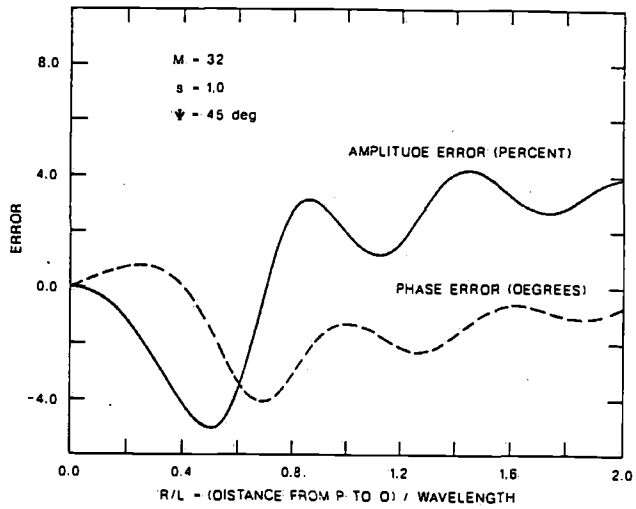

Fig.10 Cross Spectrum Errors for Wave Model 3 versus R/L.

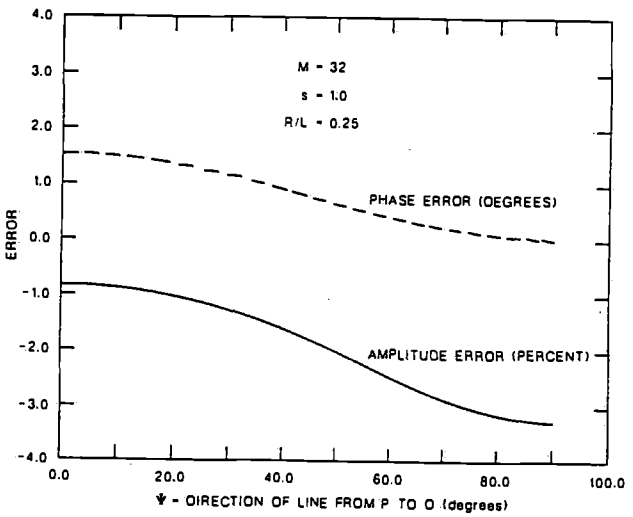

Fig.11 Cross Spectrum Errors for Wave Model 3 versus Ψ.